*International Journal of Marine Engineering Innovation and Research, Vol. 9(2), June. 2024. 378-386*
*(pISSN: 2541-5972, eISSN: 2548-1479)*



# Implementation of Kaplan Type Ducted Propeller on Hydrodynamics of Offshore Supply Vessel (OSV)

Gedhe Angkoso Nur Sofa Sakti[1], Arif Winarno[2]
(Received: 07 June 2024 / Revised: 16 June 2024 /Accepted: 19 June 2024)

***Abstract*— When operating at sea, a reliable ship must meet the planned service speed using a propulsion system. One type of propulsion system used is a ducted propeller, which is a type of propeller equipped with a channel in the form of a foil that surrounds the propeller to form a tube (nozzle). This nozzle has the ability to increase the value of thrust and torque, so that its application can increase thrust and torque compared to a propeller without a nozzle. This study aims to determine the application of the kort nozzle with MARIN foil nozzle types 19A, 22, 24 on the Ka-40 propeller on the Offshore Supply Vessel (OSV) ship using the Computational Fluid Dynamic (CFD) method. This study obtained results from all models with the model with the highest thrust force is the 19A nozzle model with a value of 367,413.41 N, while the model with the lowest thrust force is model 24 with a value of 356,314.9 Nm. From these results, it can be concluded that the relationship between the length of the nozzle cort and the thrust force is inversely proportional, that is, the greater the length of the nozzle cort used, the smaller the thrust force value produced. Likewise, the relationship between the length of the nozzle cort with torque is also inversely proportional, that is, the greater the length of the nozzle cort used, the smaller the torque value produced.**

*Keywords—Propeller Kaplan, MARIN Nozzle, Thrust, Torque*

## I. INTRODUCTION

In the upstream oil and gas industry operating in offshore areas, vessels play an important role in supporting platform operations. Offshore Supply Vessel (OSV) is one type of vessel used to support offshore platform activities [1]. The function of OSV is crucial in offshore drilling activities, especially in providing logistics supply to the platform. This type of vessel must meet optimal seaworthiness standards, be safe in maneuvering, and have high strength. This ensures the vessel can operate nimbly, safely, easily controlled, and withstand extreme conditions [2].

An important strategy in achieving this goal is to choose the optimal propulsion system according to the plan that has been developed. One alternative to increase the thrust force and propulsion efficiency of a ship is to install a cort nozzle on the propeller. This tool aims to reduce energy loss from the propeller during ship operation [3]. Kort nozzle is a plate-shaped propeller protector resembling a foil. Its function is to increase and concentrate the flow of water towards the propeller, thus maximizing the volume of water sucked by the propeller [4]. The greater the ship speed, the greater the Reynolds number. The water flow pattern before entering the hull area is still laminar, when there is an increase in ship speed the water flow pattern tends to experience turbulence [5][6]. A good hull design should minimize the resistance that occurs when the ship is operating to achieve the desired speed. A good hull design will also have many advantages, one of which is the advantage in terms of hydrodynamics [7].

The main purpose of installing a kort nozzle is to maximize the performance of the propeller, so that the thrust produced is optimal. Thrust is the force generated from the lift or lift of the rear of the propeller that moves in the same direction as the ship's motion. To get the optimal thrust and thrust force, the number of blades (leaves), pitch, and propeller leaf profile must all be considered [8]. The close proximity of the propeller shaft is also included in the factors that cause the water flow from the bow of the ship to the stern to be more collected, increasing the efficiency of the propeller thrust force [9].

With the kort nozzle or duct surrounding it, the thrust of the propeller will increase. In addition to increasing the propeller thrust, the duct also helps to improve the shape and concentrate the flow of fluid entering the propeller, so that the water coming out has a greater pressure [10]. To increase efficiency, the design of the propeller and the inner nozzle cortex should be larger. The distance between the edge of the propeller and the inner nozzle port should not exceed 0.75 % of the propeller radius [11].

In planning a propeller design, there are various types of propellers, and each type has different characteristics to meet the needs of the ship type. Kaplan Series is one type of propeller that is excellent for large power vessels with low sailing speed [12]. Likewise, in designing the nozzle cort, the large tip clearance on the ducted propeller affects the efficiency and thrust of the propeller, thrust and torque tend to decrease as the tip clearance on the ducted propeller increases [13].

According to previous research conducted by Hermawan [14] and Ahmidila [15], the condition of the OSV 80 ship in the field of ship performance decreases,

Gedhe Angkoso Nur Sofa Sakti, Departement of Marine Engineering, Universitas Hang Tuah, Surabaya, 60111, Indonesia. E-mail: gedheangkosonss@gmail.com
Arif Winarno is Lecture of Departement of Marine Engineering, Universitas Hang Tuah, Surabaya, 60111, Indonesia. E-mail: arif.winarno@hangtuah.ac.id

due to frequent losses in the propeller so that the ship speed decreases. OSV ships also require high ship motion and thrust to support offshore oil drilling activities, this is certainly suitable for the use of nozzle cortices that can increase the thrust of the propeller [16].

After seeing these conditions, there needs to be action to find solutions to overcome these problems and improve the performance of the OSV 80 ship. In this study, it tries to find out how the length of the cort nozzle affects the thrust and torque of the kaplan propeller on the OSV ship. There are three variations with different types of nozzle cortices that are able to provide the highest thrust and torque for kaplan type propellers on OSV ships. The cort nozzle to be used is MARIN foil nozzle 19A, 22, 24 with Ka-40 propeller applied to OSV 80. MARIN foil nozzle with this type has the advantage of being easy in terms of production and has ease of fabrication [17].

## II. METODE

This research will take several steps. Here are the steps:

### *A. Problem Identification*

This research aims to provide answers to problems raised from the problems in the background which contain the conditions in the field of Offshore Supply Vessel 80 (OSV) ships often occur losses so that the ship's speed decreases.

### *B. Literature Study*

In this step, the aim is to obtain a summary of the current theoretical basis, as well as additional references and information to support it.

- *Force drag and force lift*

  According to Popov, drag and lift forces are created when the stress is multiplied by the stress area. However, the sum of these forces must remain equal or balanced on an imaginary object [18]. Shear stress, represented by the symbol "τ" (tau), is an additional component of the intensity of the force acting parallel to the base plane area. It can be defined mathematically as follows:

$$\tau = \lim_{A \to 0} \frac{\Delta V}{\Delta A} \quad (1)$$

  Therefore, the mathematical formula of the drag force from the above equation can be written as follows:

$$F_{drag} = \tau \, x \, A \quad (2)$$

  However, the mathematical formula of the lift force from the above equation can be obtained in the following way:

$$F_{lift} = P \, x \, A \quad (3)$$

  Where, $F_{Drag}$ is drag, $F_{Lift}$ is lift, τ is wallshear, P is pressure and A is Area.

- *Thrust and Torque*

  To calculate the forces acting on a propeller or turbine, blade element momentum theory combines blade element theory and momentum theory. The combination of these two theories helps overcome some of the problems in calculating the rotor speed generated, as shown in figure 1 [19].

  The thrust force utilizes the propeller to push the ship into motion. The momentum blade element theory, which combines blade element theory and momentum theory, can be used to calculate the force acting on the propeller. To do so, we can use the following equation to find the force acting on the propeller.

$$F_Z = F_L \cos\theta - F_D \sin\theta \quad (4)$$

$$F_X = F_L \sin\theta + F_D \cos\theta \quad (5)$$

  From the blade momentum element theory equation, the thrust force equation is as follows:

$$T = F_{Lift} \cos\theta - F_{Drag} \sin\theta \quad (6)$$

  Where, T is thrust and θ is pitch.

  The twisting ability of an object (propeller) that causes the object to rotate on its axis is called torque. Torque can be calculated by multiplying the force (F) and moment arm, so it can be written:

$$\tau = F \, x \, r \quad (7)$$

  Where is the torque, F is the force, r is the moment arm.

  Therefore, the momentum equation, if torque is acting on a blade, can be found using blade element theory:

$$Q = (F_{Lift} \cos\theta + F_{Drag} \sin\theta) \, x \, r \quad (8)$$

  Where Q is torque and θ is pitch.

  To calculate thrust and torque, it is necessary to know the pitch angle by utilizing the P/D value previously determined. Therefore, based on these values, the pitch angle obtained is:

$$\theta = tan^{-1} \frac{P/D}{0{,}7\pi} \quad (9)$$

### *C. Collecting Data*

Based on the data obtained from the data collection process in previous studies, this study uses the Offshore Supply Vessel object, with the Kaplan Ka-40 propeller and for the nozzle cort ordinate data using the MARIN foil nozzle obtained from the MARINE PROPELLERS AND PROPULSION book by John Carlton [17].

### *D. Modelling*

After obtaining the necessary data, the next step is modeling. 2D modeling uses autocad software and 3D modeling is done using rhinoceros software.

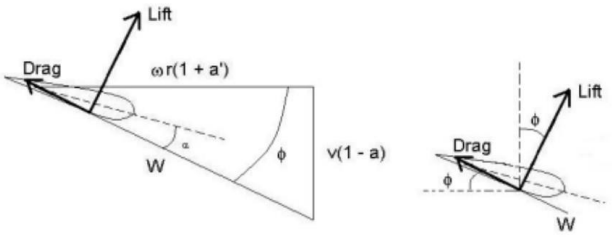


Figure 1. Force Acting on The Blade

*E. Computational Fluid Dynamics*

The next step is to simulate using Ansys Fluent with meshing. The project scheme consists of geometry, mesh, setup, solution, results.

## III. Result and Discussion

*A. Principal Dimensions*

Offshore Supply Vessel 80 (OSV) ship data is data obtained in previous studies. The following are the main ship sizes and ship types as in table 1.

Tabel 1.
Principal Dimensions

| Parameter | Symbol | Offshore Supply Vessel 80 |
|---|---|---|
| Overall length (m) | Loa | 40,000 |
| Length of waterline (m) | Lwl | 38,000 |
| Length between upright lines (m) | Lbp | 36,800 |
| Maximum width (m) | B | 11,400 |
| Height (m) | H | 4,950 |
| Draft (m) | T | 4,000 |
| Service speed (knots) | $v_d$ | 13,000 |

*B. Propeller Data*

Based on the previously collected data, the model to be selected to be equipped with a nozzle is the Ka-40 propeller with a rake of 5°. This propeller dimension reflects the best specification based on previous research results. Therefore, based on the existing data, the propeller model will be built with a nozzle.

The process begins with modeling the Ka-40 propeller according to the predetermined parameters, then continues with modeling the Ka-40 propeller with the addition of a nozzle. This process starts with detailing all aspects, including the extended blade, pitch diagram, develop and project outline, and side view, the dimensions of the Kaplan propeller as listed in table 2.

Tabel 2.
Propeller Data

| No. | Propeller dimension Ka-40 rake $5^o$ | |
|---|---|---|
| 1 | Type | Ka-40 |
| 2 | Diameter | 2,4 m |
| 3 | Efficiency | 0,56 |
| 4 | Round | 300 rpm |
| 5 | Pitch | 0,65 |

*C. Kort Nozzle Data*

After the propeller model geometry drawing process is complete, the next step is to draw the nozzle model geometry. Nozzle ordinate data can be obtained from book references [17]. This ordinate data describes the percentage of the Ld (duct length) value. as shown in table 3.

Tabel 3.
Kort Nozzle Data

| Ordinate No. 19A-24 | | | L/D Nozzle | |
|---|---|---|---|---|
| *x/L* | *yi/L* | *yu/L* | 19A | 0.5 |
| 0 | 18,25 | 0 | 22 | 0.8 |
| 1,25 | 14,66 | 20,72 | 24 | 1.0 |
| 2,5 | 12,8 | 21,07 | | |
| 5 | 10,87 | 20,8 | | |
| 7,5 | 8 | | | |
| 10 | 6,34 | | | |
| 15 | 3,87 | | | |
| 20 | 2,17 | | | |
| 25 | 1,1 | | | |
| 30 | 0,48 | *straight* | | |
| 40 | 0 | *line* | | |
| 50 | 0 | | | |
| 60 | 0 | | | |
| 70 | 0,29 | | | |
| 80 | 0,82 | | | |
| 90 | 1,45 | | | |
| 95 | 1,86 | 6,36 | | |
| 100 | 2,36 | 6,36 | | |

*D. Modelling*

The geometry of the Offshore Supply Vessel 80 (OSV) hull and Kaplan propeller using AutoCAD software from data obtained from previous research [2][14], as shown in Figure 2 and Figure 3.

The first stage before the simulation process using Computational Fluid Dynamic software is the OSV ship model. In making the model in the design using autocad software in the form of 2 dimensions and making 3D models using rhinocerros software as shown in Figure 4.

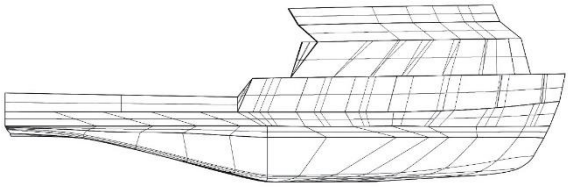

Figure 2. 2D Geometry of OSV

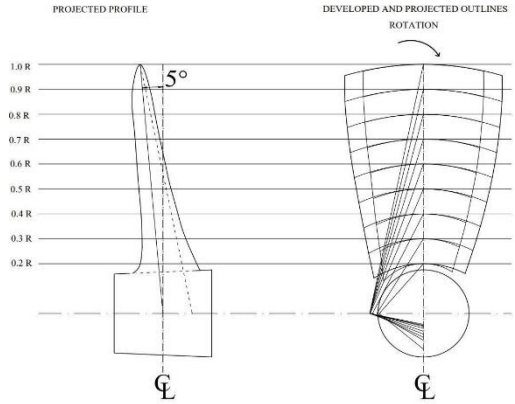


Figure 3. 2D Geometry of Ka-40 rake 5°

Figure 5, Figure 6, and Figure 7 show the geometry of the Kort nozzle model types 19A, 22, 24 that have been combined with the Kaplan propeller using rhinoceros software.

*E. Geometry*

In the geometry stage, the first step is to import the models from Rhinoceros software into SpaceClaim software in Ansys. After all models have the right surface, the next step is to create an experimental domain. In this research, the experimental domain is divided into 2, static domain and rotating domain. The static domain is pool-shaped and acts as a testing area where fluid phenomena around the hull can be observed. The dimensions of this domain are further described in Figure 8 and Table 4 [2].

TABEL 4.
DOMAIN STATIC DIMENSION

| Name | Description | Length (mm) |
|---|---|---|
| L1 | Length from bow to leading edge of domain (Lpp x 4) | 120.000 |
| L2 | Length from stern to back side of domain (Lpp x 3) | 160.000 |
| L3 | Length from stern to bottom of domain (Lpp x 2.5) | 80.000 |
| L4 | Length from stern to left and right sides of the domain (Lpp x 2) | 100.000 |

The rotating domain is an area surrounding the propeller that will be defined in a rotating state. Figure 9 shows the dimensions of the rotating domain [20].

*F. Meshing*

After the fluid domain is formed, the next step is meshing. In this study, the application of meshing is divided into two parts with different meshing sizes (add local sizing), namely the propeller and duct parts and the outside or where the fluid is read. For facesize 0.035 m and curvature 0.0035 m. At a minimum size of 0.05 m generate the surface mesh, while the maximum is 1 m. Improve surface mesh is also used to correct the skewness of the mesh by 0.6. Regions of static domain and rotating domain are defined as fluid. Poly-hexcore is used for the volume mesh so that the number of cells formed is not too much [21]. The number of cells formed as many as 1,934,020 cells can be seen in Figure 10.

*G. Setup*

This setup stage is related to the configuration of simulation parameters. In this setup stage, simulation parameters are adjusted to various conditions, including inlet, wall, outlet, ship, duct and propeller boundaries as the model to be tested. In the inlet condition, the incoming fluid flow is defined, as well as the outlet which is the outgoing fluid flow. The wall boundary condition indicates the pool boundary at the bottom, and sides, while the ship refers to the surface of the hull that can affect the fluid flow in the simulation. The solver used is preasure-based steady, Reynold stress for viscous models because it is suitable for rotating systems [22]. In the cell zone conditions, the rotating domain is defined as liquid water (with a rotational velocity of 300 rpm) as well as the static domain. Velocity at the inlet is 6.68778 m/s or 13 knots and the propeller is a rotational moving wall for boundary conditions.

*H. Solution*

After completing the setup in the program, the next step is to perform the solution. The solution process involves calculations that are performed iteratively after completing the setup with a total of 1000 iterations. The results of the solution process can be seen in Figure 11, which displays a graph with the x-axis showing iterations, and the y-axis showing thrust in units of Newton (N) and Figure 12 showing torque (Nm).

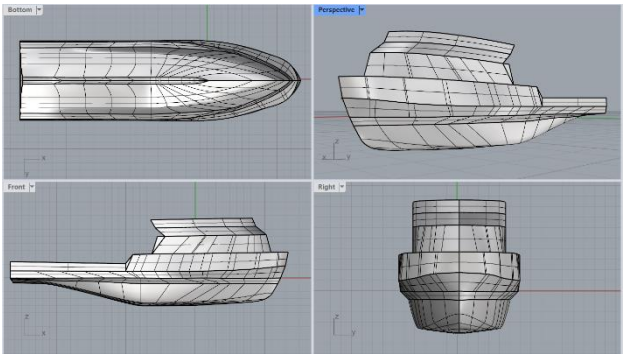

Figure 4. 3D Geometry of OSV

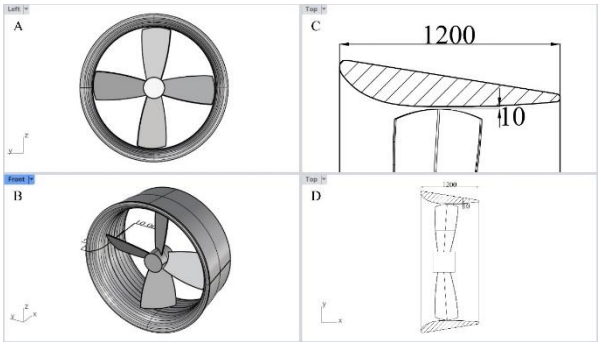


Figure 5. Geometry of Kort Nozzle Model 19A

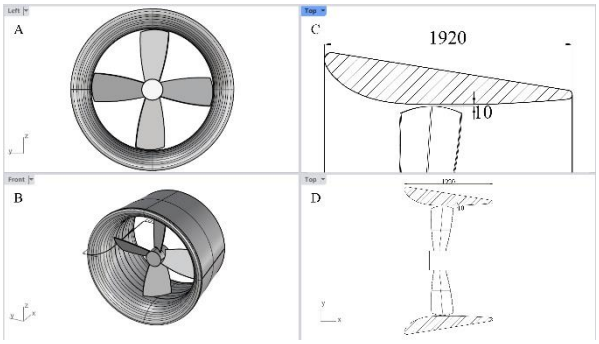


Figure 6. Geometry Of Kort Nozzle Model 22

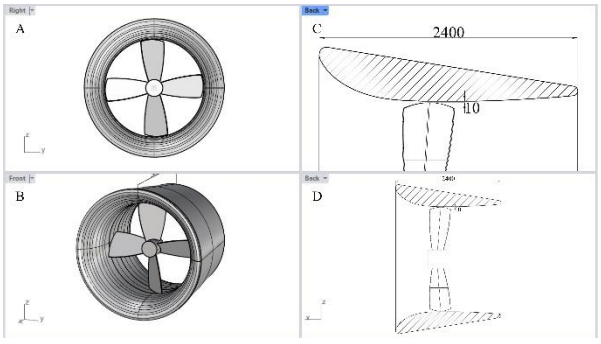


Figure 7. Geometry of Kort Nozzle Model 24

### *I. Result*

Result is the stage where visualization of simulation results can be seen from the desired point of view. This visualization can include a description of the flow, pressure, temperature, or velocity in the model that has been given variable variations. Figure 13 illustrates the flow velocity distribution behind the ship. The highest velocity, reaching 19.117 m/s, occurs behind the propeller and is shown in yellow in the figure. As it moves away from the propeller, the flow velocity begins to decrease to 9.033 m/s, and as it moves further away from the propeller, the flow velocity continues to decrease until it reaches 0 m/s.

Figure 14 shows the fluid flow contours in the fluid domain. It can be seen that the flow rotates due to the rotating propeller model, and due to the duct on the propeller, the flow is focused in the center.

Figure 15 also shows the pressure contours that occur in the fluid flow around the propeller and cort nozzle. From the figure it can be seen that the higher pressure is on the outside of the cort nozzle. This is because the fluid flow velocity on the outside of the nozzle is lower than the inside of the nozzle.

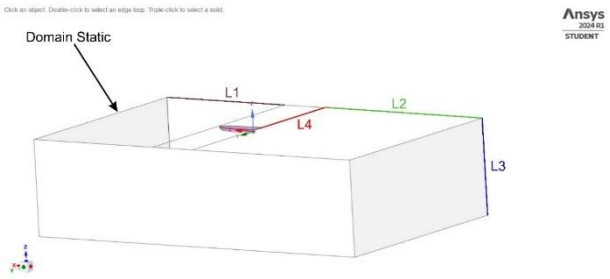


Figure 8. Domain Static

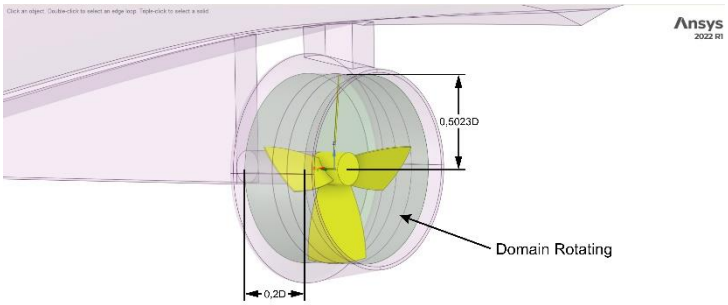


Figure 9. Domain Rotating

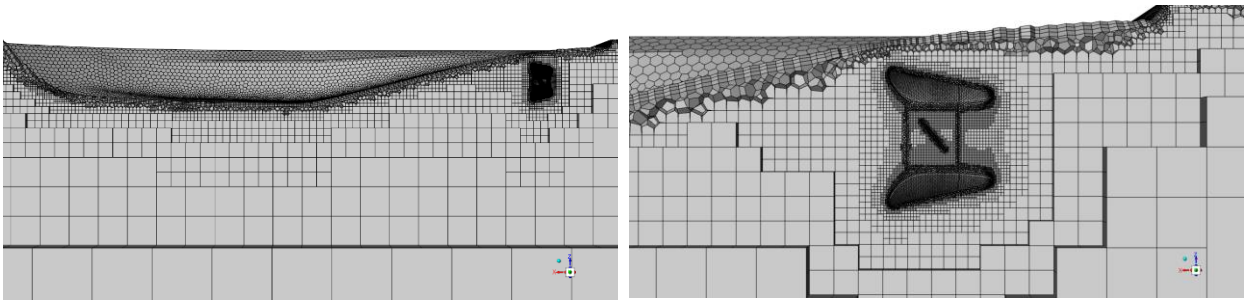

(a) (b)

Figure. 10. Meshing result of kort nozzle (a) hull (b) ducted propeller

*J. Data Processing*

Calculations were carried out using simulated data to determine the performance of the propeller, in accordance with the objectives of this study, which is to evaluate the performance of the ducted propeller.

- Thrust calculation

In accordance with the propeller data, the P / D value of the propeller is 0.65. Then the pitch angle value can be calculated with the following equation [23]:

$$\theta = tan^{-1}\frac{P/D}{0,7\pi}$$

$$\theta = tan^{-1}\frac{0,65}{0,7\pi}$$

$$\theta = 16,47°$$

The lift and drag forces are obtained from the CFD post simulation results. The thrust force value, which will be displayed in the graph, is obtained by calculating the lift and drag force according to equation (6), as well as the pitch angle value obtained.

- Torque calculation

The torque value is obtained from equation (8), the lift and drag are taken from the simulation results read by the calculator function. The torque value taken is the value perpendicular to the propeller axis.

The results of the simulation process need to be validated with the calculation of thrust and torque that has been done numerically. Table 4.3 shows the thrust value between Ansys simulation and numerical

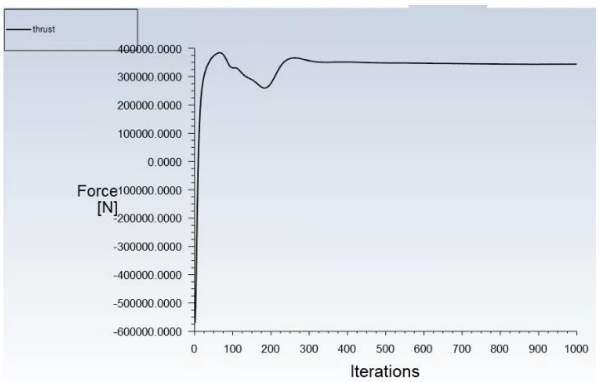


Figure 11. Results of solution thrust kort nozzle 19A

calculation. There is a difference between the thrust value produced in the Ansys simulation and the results of manual calculations, where the thrust value in the Ansys simulation tends to be lower than the manual calculation. Table 4.3 also indicates that the average difference between the two values is around 2-4% for each model variation.

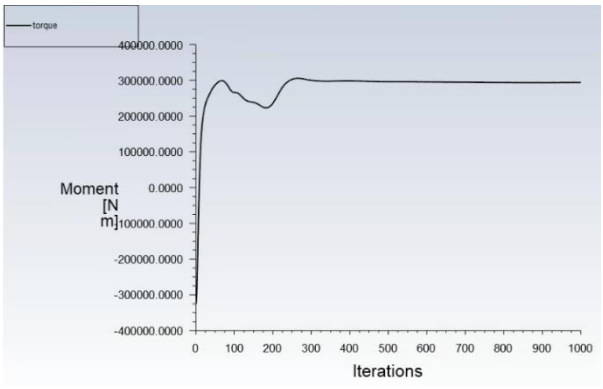


Figure 12. Results of Solution Torque Kort Nozzle 19A

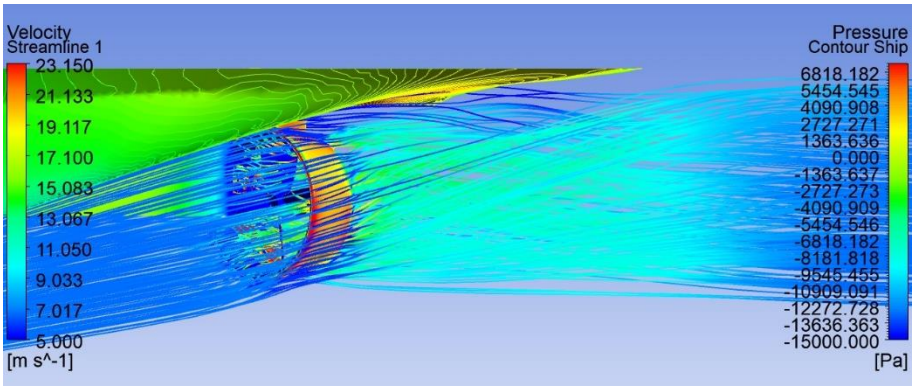


Figure 13. Velocity Streamline of Kort Nozzle 19A

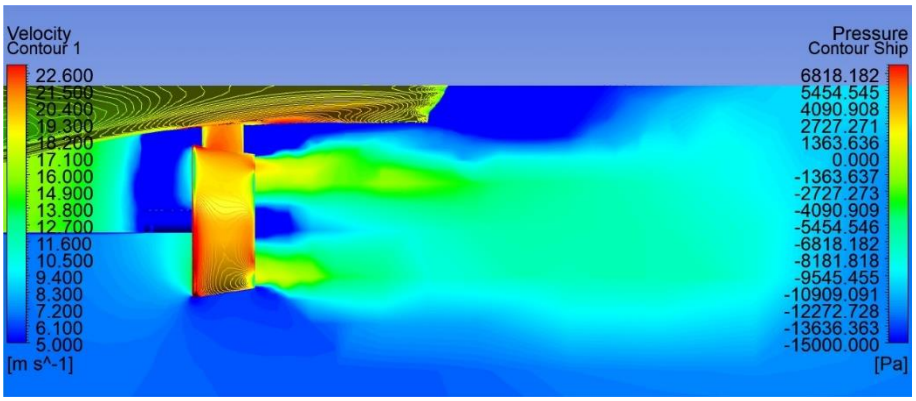


Figure 14. Velocity Contour of Kort Nozzle 19A

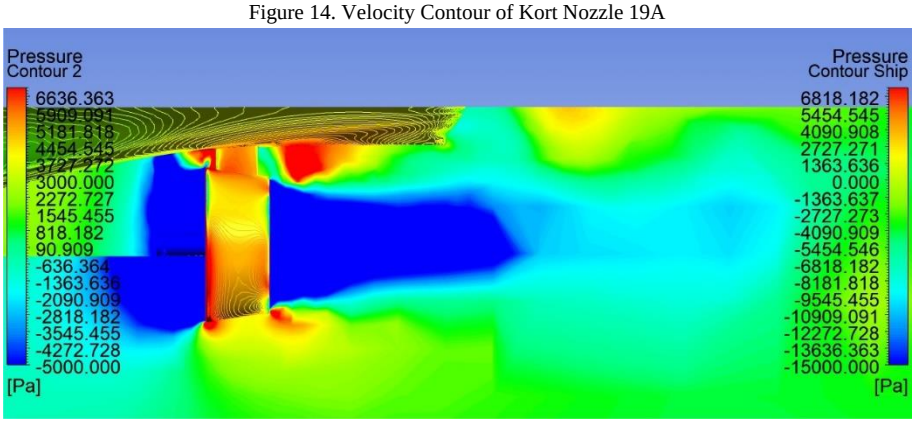


Figure 15. Pressure Contour of Kort Nozzle 19 A

TABEL 5.
COMPARISON OF NUMERICAL CALCULATION AND CFD SIMULATION (A) THRUST (B) TORQUE

(A)

| Model | Numerical Calculation (N) | CFD Simulation (N) | Difference (%) |
|---|---|---|---|
| 19A | 357.513,43 | 367.413,41 | 2,69 |
| 22 | 353.991,60 | 365.484,15 | 3,14 |
| 24 | 350.920,95 | 365.027,80 | 3,86 |

(B)

| Model | Numerical Calculation (N) | CFD Simulation (N) | Difference (%) |
|---|---|---|---|
| 19A | 308.691,04 | 315.338,05 | 2,10 |
| 22 | 301.704,85 | 309.948,68 | 2,65 |
| 24 | 294.997,57 | 309.126,03 | 4,57 |

In Table 5, the thrust and torque results from simulation and numerical calculations are shown. The difference is less than 5% in each model variation. This shows that the thrust and torque results from the Computational Fluid Dynamics (CFD) simulation approach and numerical calculations are not significantly different [24]. Model 19A has the highest thrust and torque values, while model 24 has the lowest thrust and torque values.

Furthermore, the calculation results of each model will be converted into graphs from table 5. This allows an understanding of the characteristics of each simulated model. The comparison between each model against thrust and torque is shown in figure 16.

In the comparison graph of thrust and torque on models 19A, 22, 24 shows that the greater the length of the nozzle cort the value of thrust and torque decreases.

With these results, each cort nozzle model compared to model 19A is the most effective for increasing thrust and torque because it is able to get the largest thrust and torque results. Therefore, it can be concluded that the use of a cort nozzle greatly affects the results of thrust and torque.

## IV. CONCLUSION

1. The relationship between nozzle cortex length and thrust is inversely proportional, where the greater the length of the nozzle cortex used, the smaller the thrust value produced.
2. The relationship between cort nozzle length and torque is also inversely proportional, where the greater the length of the cort nozzle used, the smaller the torque value produced.

Further research can be done by conducting research on variations in the angle of attack of the cort nozzle to find out the hydrodynamic characteristics of these differences. In addition, further research can also include wind and current factors in the research object.

## Acknowledgements

We would like to express our gratitude to Hang Tuah University Surabaya for the support provided for this research. We would also like to express our appreciation to the fluid laboratory team for the assistance and facilities provided to carry out this research.

## REFERENCES

[1] S. A. Robby, 2018, "Model Optimasi Penjadwalan Offshore Support Vessel : Studi Kasus Wilayah Operasi Laut Natuna Selatan," Institut Teknologi Sepuluh November.
[2] M. H. Firmansyah, 2023, "Studi Perbandingan Penerapan Haluan Axe Bow Dengan Ulstein X-Bow Pada Kapal Offshore Supply Vessel (OSV) 80 Terhadap Hambatan Total," Universitas Hang Tuah.
[3] A. F. Rachmat, A. Trimulyono, and P. Manik, 2021, "Analisa Pengaruh Pemasangan Energy Saving Device (ESD) Jenis Mewis Duct Terhadap Thrust Propeller INSEAN E779A Dengan Menggunakan Pendekatan CFD," Jurnal Teknik Perkapalan, vol. 9, no. 3,pp. 294–302.
[4] A. T. Januar and A. Winarno, 2023, "Pengaruh Penerapan Energy Saving Device (ESD) Kort Nozzle untuk Meningkatkan Gaya Dorong Propeller pada Kapal Ikan Purse Seine," Saintara: Jurnal Ilmiah Ilmu-Ilmu Maritim, vol. 7, no. 1, pp. 11-17.
[5] A. Winarno, G. Ciptadi, A. Iriany, and A. S. Widodo, 2023, "Experiment Study of the Resistance on Nusantara Ship Hull Modification with Fishing Boat in Pantura East Java," International Journal on Engineering Applications, vol. 11, no. 2, pp. 111–120.
[6] A. Winarno, G. Ciptadi, A. Iriany, and A. S. Widodo, 2023, "Experimental and Numerical Study of Ship Resistance on the Combination of Traditional Nusantara Fishing Vessel Hull Forms," International Review of Mechanical Engineering, vol. 17, no.4 , pp. 190–196.
[7] G. A. Putra and A. Winarno, 2022, "Studi Pengaruh Variasi Bentuk Wave-Piercing Terhadap Hambatan Pada Kapal Katamaran Untuk Meningkatkan Efisiensi Pemakaian Bahan Bakar," Zona Laut: Jurnal Inovasi Sains dan Teknologi Kelautan, vol. 3, no.1, pp. 24-31.
[8] D. N. Yunita and A. Winarno, 2019, "Analisa Teknis Pengaruh Jumlah Sudu Propeller Bebas Putar Terhadap Gaya Dorong Kapal Tunda DPS Ix," Seminar Nasional Kelautan XIV: Implementasi Hasil Riset Sumber Daya Laut dan Pesisir Dalam Peningkatan Daya Saing Indonesia.
[9] M. F. Rozi and A. Winarno, 2019, "Pengaruh Variasi Jarak Poros Propeller Yang Berbeda Pada Kapal Ikan Tradisional KM. Sri Mulyo di Brondong Lamongan," Seminar Nasional Kelautan XIV: Implementasi Hasil Riset Sumber Daya Laut dan Pesisir Dalam Peningkatan Daya Saing Indonesia.
[10] F. Rozzaq, 2013 "Penentuan Jenis Kort Nozzle Pada Kapal Tunda DPS IX," Universitas Hang Tuah.
[11] H. Schneekluth and V. Betram, 1998, "Ship Design for Efficiency and Economy," Oxford : Butter Worth Heinmann.
[12] M. D. Maulana, A. F. Zakki, and P. Manik, 2020, "Analisa Performance Propeller Tipe KA4-70 dengan Variasi Flap Angle End Plate dan Sudut Rake," Jurnal Teknik Perkapalan, vol. 8, no. 1, pp. 11–20.
[13] D. Yongle, S. Baowei, and W. Peng, 2015, "Numerical Investigation of Tip Clearance Effects on The Performance of Ducted Propeller," Int. J. Nav. Archit. Ocean Eng., vol. 7, pp. 795-804.
[14] M. A. R. Hermawan and A. Winarno, 2023, "Kajian Teknis Propeller Tipe B - Series Dan Kaplan Dengan Variasi Sudut Rake Pada Kapal Offshore Supply Vessel 80 (OSV 80)," Zona Laut: Jurnal Inovasi Sains dan Teknologi Kelautan, vol. 4, no. 3, pp. 309-318.
[15] W. N. R. Ahmidilla, 2024, "Analisa Penerapan Kort Nozzle Untuk Propeller B4-40 Kapal Offshore Supply Vessel (OSV)," Univeristas Hang Tuah.
[16] P. I. Adyanata and A. Winarno, 2022, "Kajian Teknis Penggunaan Hub dan Hubless Rim Driven Propeller (Rdp) Sebagai Propeller Kapal Di Perairan Dangkal," Jurnal Inovtek Polbeng, vol. 12, no. 1.
[17] J. Carlton, 2007, "Marine Propellers and Propulsion," Oxford : Elsevier Ltd. All right reserved.
[18] E. P. Popov, 1984, "Mechanic of Materials." San Francisco. Berkeley.
[19] T. B. Musriyadi, Amiadji, and B. S. Cahyono, 2017, "Technical Analysis of Kort Nozzle Application for SPOB Ship 4990 DWT on River," International Journal of Marine Engineering Innovation and Research, vol. 1, no. 3, pp 168-174
[20] X. Zhang, Z. Liu, L. Cao, and D. Wan, 2022, "Tip Clearance Effect on The Tip Leakage Vortex Evolution and WakeInstability of a Ducted Propeller," J. Mar. Sci. Eng.
[21] Ansys, 2020, "ANSYS Fluent Mosaic Technology Automatically Combines Disparate Meshes with Polyhedral Elements for Fast, Accurate Flow Resolution," Ansys, Inc. All Rights Reserved.

[22] F. R. Menter, R. Lechner, and A. Matyushenko, 2021, "Best Practice: RANS Turbulence Modeling in Ansys CFD," Ansys, Inc. All Rights Reserved.
[23] I. S. Arief, T. B. Musriyadi, and A. D. A. J. Mafera, 2017, "Analysis Effect of Duct Length– Nozzle Diameter Ratio and Tip Clearance Variation on the Performance of K-Series Propeller," International Journal of Marine Engineering Innovation and Research, vol. 2, no. 1, pp. 77-85.
[24] A. Winarno, A. S. Widodo, G. Ciptadi, and A. Iriany, 2024, "The Effect of Sail Layout on Fishing Vessels Hydrodynamics in the North Coast of Java using Computational Fluids Dynamic," Semarak Ilmu: CFD Letter, vol. 16, issue. 1, pp. 107-120.